

# Applications of Knot Theory to Magnetohydrodynamics

Ishaan Singh Chandok

August 21, 2020

## 1 Introduction

From the very small superfluid vortices to magnetic flux tubes that can be found in the Sun, knots and links appear embedded in fluids on varying orders of magnitude [7]. Fluid dynamics studies the motion of fluids, often treating it as a dynamical systems problem. Focusing on the position of fluid particles with respect to time makes the study of concepts such as turbulence mathematically and computationally demanding. Topological fluid dynamics aims to simplify the study of fluids by instead focusing on invariants of flow.

In this paper, we treat embedded fluid structures as collections of flux tubes and study invariants of their motion. We find that helicity, a physical invariant, has a connection to linking number, an invariant in knot theory. We then study the relaxation of magnetic fields under the constraint that they must deform via ambient isotopy. Due to the invariance of knot topology, volume, and flux, we can show that there must be positive lower bound to the potential energy of a magnetic field embedded in a fluid.

## 2 Prerequisite Knowledge from Knot Theory

A **topological embedding** of  $A$  into  $X$  is a map  $f : A \rightarrow X$  such that  $f$  is injective, continuous, and is a homeomorphism onto its image (with the subspace topology) [10]. A map  $f$  between topological spaces is a **homeomorphism** when it is continuous with a continuous inverse. In fluid dynamics, we treat concepts such as vortices as manifolds to ignore the effects of molecular structure. An  **$n$ -manifold** is a topological space such that for every point, we can find a neighbourhood homeomorphic to  $R^n$ . A **diffeomorphism** is a map  $f$  between manifolds such that  $f$  and its inverse are differentiable. As we will prove, a distortion of a manifold embedded in a fluid medium occurs by means of a diffeomorphism.

A **knot** is an embedding of the circle  $S^1$  into  $R^3$ . Two important examples of knots are the unknot and the trefoil knot (Figure 1):



Figure 1: Left: Unknot, Right: Trefoil Knot, from [4]

A **link** is an embedding of a collection of circles [9]. The number of **components** of the link equals to the number of circles we embed into  $R^3$ , meaning a knot is a one-component link. A

diagram to visualize the links is known as a **projection**. We denote crossings of components by keeping one line solid at an intersection and breaking the other. For example, the Hopf link is formed by embedding two unknots as displayed in Figure 4.

A goal of knot theory is determining which knots can be continuously deformed into the unknot. The notion of deformation is defined via a concept known as ambient isotopy.

**Definition.** Let  $f$  and  $g$  be embeddings of  $S^1$  into  $R^3$ , defining two knots. These knots are equivalent via ambient isotopy if there exists a continuous function  $H : R^3 \times [0, 1] \rightarrow R^3$  such that  $H_0 \circ f = f$ ,  $H_1 \circ f = g$ , and each  $H_t$  is a homeomorphism.

A concise definition of ambient isotopy is to call it a ‘homotopy of homeomorphisms’ [8]. Ambient isotopy defines an equivalence class on the diagrams of knots, and intuitively means to continuously deform the knot without cutting it [8].

The rules for deforming the projections of links are summarized by the **Reidemeister moves**. According to Kauffman, two knot or link diagrams are ambient isotopic if and only if we can relate them by Type I, II, and III Reidemeister moves [9]. Taking this theorem as a given, the three types of Reidemeister moves are shown in Figure 2.

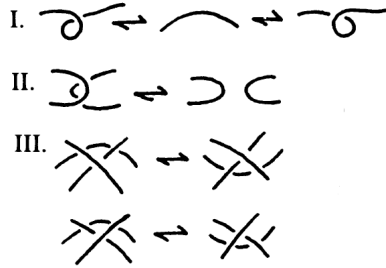


Figure 2: Reidemeister Moves, from [9]

Type I moves are characterized by an ‘untwisting’ motion in a single component. Type II moves can be visualized as ‘poking/unpoking’ the strand of one component into another. Type III moves represent the sliding of one strand over the others [4].

Knot theory offers a method to compute how ‘linked’ components are using the **linking number**. To compute the linking number, we must choose a projection of our link, focusing on two components. Then, we assign signs to each crossing of the two components we are focusing on according to Figure 3. The linking number is obtained by taking the sum of every contribution of the crossings and dividing this by 2.

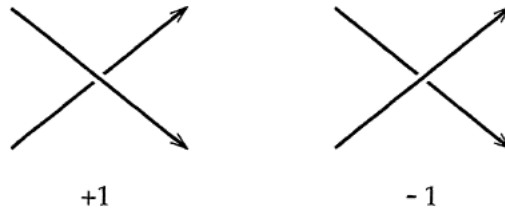


Figure 3: Signs based on Crossing Type, from [4]

**Example (Hopf Link).** In Figure 4, we assign the signs for every crossing to a Hopf link. We find that the sum of the contributions of every crossing is  $+2$ . Dividing this number by 2 shows that the linking number of the Hopf link is 1. Note that if we changed the direction of one arrow (i.e. flipped the orientation of one component), the linking number would become  $-1$ . If we changed the direction of both arrows, it would be 1 [4].

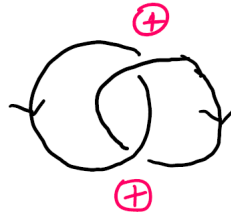


Figure 4: Hopf Link

**Example (Whitehead Link).** We can also compute the linking number of the Whitehead link. Shown in Figure 5 is a projection of the Whitehead link with the signs of the crossings labeled. We see that the linking number must be 0. This is interesting as it shows that multi-component links need not have a non zero linking number.

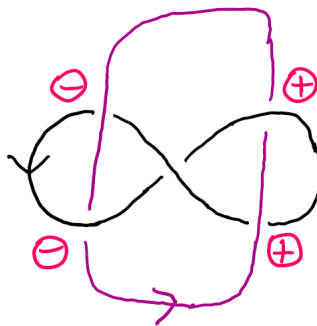


Figure 5: Whitehead Link

**Theorem.** Linking number is a link invariant, meaning it is invariant under ambient isotopy.

*Proof.* (From [4]) Looking at Type I Reidemeister moves, these alter the ‘self-crossing’ of a single component. However, Type I moves do not affect how a component crosses with other components, hence it leaves the linking number unchanged.

A Type II move removes/introduces a pair of crossings with opposite signs (one is  $+1$ , one is  $-1$ , so they cancel each other out). Figure 6 shows that there is no total change in Linking Number under Type II moves.

A Type III move does not change the number of  $+1$  and  $-1$  intersections in the diagram (Figure 7). Therefore, it has no effect on the linking number.

Since linking number is not affected by Type I, II, and III Reidemeister moves, it must be a link invariant.  $\square$

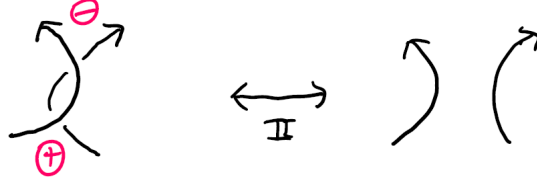


Figure 6: Linking Number Invariant under Type II Move

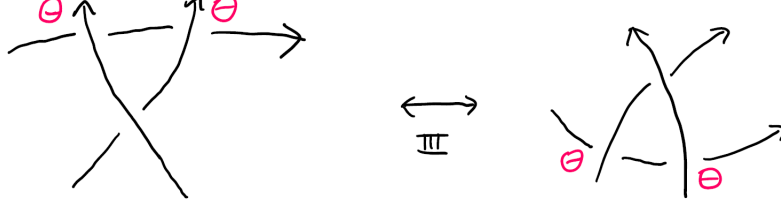


Figure 7: Linking Number Invariant under Type III Moves

Given a knot, a **flux tube** is defined by placing a cylindrical tube around the knot. The knot is the centre-line of the flux-tube, which encloses volume  $V$  and has flux  $\Phi$ . In Section 4, we treat the magnetic field as a collection of possibly linked flux tubes and show that the deformation of these tubes occurs via ambient isotopy.

### 3 Prerequisite Knowledge from Fluid Dynamics

Fluid dynamics deals with the flow of fluids mostly under continuous distortions. The aim of this section is to define helicity, a physical invariant of the Euler equations.

Consider an ideal (incompressible and inviscid) fluid of constant density. Let  $\mathbf{u}(\mathbf{x}, t)$  denote the velocity field of this fluid. The Euler equations (1 & 2) are a simplified case of the Navier-Stokes equations obtained by neglecting the effects of internal friction.

$$\frac{\partial \mathbf{u}}{\partial t} + (\mathbf{u} \cdot \nabla) \mathbf{u} = -\frac{1}{\rho} \nabla p \quad (1)$$

$$\nabla \cdot \mathbf{u} = 0 \quad (2)$$

Where  $\rho$  denotes density and  $p$  is pressure.

By embedding some fluid structure in this field, we get  $\omega(\mathbf{x}, t)$  a vorticity field satisfying  $\omega = \nabla \times \mathbf{u}$  and  $\nabla \cdot \omega = 0$ . As described previously, a goal of the paper is to understand these vortices using knot theory. Under Euler evolution, vortices embedded in an ideal fluid are not subject to dissipative effects, and satisfy the ‘frozen field’ property (Equation 3).

$$\frac{\partial \omega}{\partial t} = \nabla \times (\mathbf{u} \times \omega) \quad (3)$$

The ‘frozen field’ property is a result of Helmholtz’s laws of vortex motion, which claims that the flux velocity of vortex lines is preserved during their transport through a fluid [1].

An important physical property of a vorticity field is its **helicity**. By definition, helicity,  $\mathcal{H}$ , measures how knotted and complex the vortex lines are [2], being defined as:

$$\mathcal{H} = \int \mathbf{u} \cdot \boldsymbol{\omega} dV \quad (4)$$

**Theorem.** Given a fluid with a velocity field  $\mathbf{u}$  satisfying Euler's equations, provided the field decays sufficiently fast at the boundary (i.e.  $\mathbf{u}$  approaches 0 as we reach the boundary), then helicity is an Euler invariant.

*Proof.* (From [6]) Suppose  $\mathbf{u}$  is defined in  $S \subseteq R^3$ . The time derivative of helicity is written as:

$$\frac{d\mathcal{H}}{dt} = \frac{d}{dt} \int_S \mathbf{u} \cdot \boldsymbol{\omega} dV$$

By the Leibniz Integration Rule, we can distribute this derivative into the integral. Combined with the product rule for dot products, we get:

$$= \int_S \frac{\partial \mathbf{u}}{\partial t} \cdot \boldsymbol{\omega} + \mathbf{u} \cdot \frac{\partial \boldsymbol{\omega}}{\partial t} dV$$

The frozen field equation (3) gives us the second partial derivative. Let  $h = \frac{p+(1/2)u^2}{\rho}$ . The first partial derivative is given by the following re-writing of the Euler equations: (We assume  $\rho$  is a constant, so the gradient term 'ignores' it).

$$\frac{\partial \mathbf{u}}{\partial t} = -\nabla h + (\mathbf{u} \times \boldsymbol{\omega})$$

Substituting the Euler equation and frozen field equation into the integral, we get:

$$\frac{d\mathcal{H}}{dt} = \int_S -\nabla h \cdot \boldsymbol{\omega} + (\mathbf{u} \times \boldsymbol{\omega}) \cdot \boldsymbol{\omega} + \mathbf{u} \cdot (\nabla \times (\mathbf{u} \times \boldsymbol{\omega})) dV$$

Since  $\nabla \cdot \boldsymbol{\omega} = 0$ , we can show that  $-\nabla h \cdot \boldsymbol{\omega} = -\nabla \cdot (h\boldsymbol{\omega})$ . Substituting  $\boldsymbol{\omega} = \nabla \times \mathbf{u}$ ,

$$\frac{d\mathcal{H}}{dt} = \int_S -\nabla \cdot (h\boldsymbol{\omega}) + (\mathbf{u} \times \boldsymbol{\omega}) \cdot (\nabla \times \mathbf{u}) + \mathbf{u} \cdot (\nabla \times (\mathbf{u} \times \boldsymbol{\omega})) dV$$

Using,

$$\nabla \cdot (\mathbf{A} \times \mathbf{B}) = \mathbf{B} \cdot (\nabla \times \mathbf{A}) - \mathbf{A} \cdot (\nabla \times \mathbf{B})$$

and factoring out the divergence operator:

$$\frac{d\mathcal{H}}{dt} = \int_S \nabla \cdot (-h\boldsymbol{\omega} + (\mathbf{u} \times \boldsymbol{\omega}) \times \mathbf{u}) dV$$

Now, we apply the divergence theorem, which states that the volume integral of the divergence equals the surface integral on the boundary. We assumed that as we approach the boundary (possibly at infinity),  $\mathbf{u}$  decays to 0, meaning  $\frac{d\mathcal{H}}{dt} = 0$ , as desired.  $\square$

## 4 Magnetohydrodynamics (MHD)

MHD deals with the magnetic fields of conducting fluids, such as plasmas. In this section, we embed a magnetic field in a fluid medium, and study the characteristics of this field through the lens of topology.

Consider a perfectly conducting and ideal fluid defined in  $D \subseteq R^3$ . Let  $\mathbf{u} = \mathbf{u}(\mathbf{x}, t)$  denote the velocity field of this fluid. Assume the fluid satisfies the Euler equations (1 & 2) and apply the boundary condition that  $\mathbf{u} = 0$  on boundary  $\partial(D)$  (possibly at infinity). Let  $\mathbf{B} = \mathbf{B}(\mathbf{x}, t)$  denote a magnetic field embedded in this fluid. We can study the ‘transport’ of  $\mathbf{B}$  from time  $t = 0$  to an arbitrary time  $t$  using the fluid flow map:

**Definition (Fluid Flow Map).** Let  $\mathbf{B}(\mathbf{a}, 0)$  denote the initial magnetic field configuration and let  $\mathbf{B}(\mathbf{x}, t)$  be some final field configuration at time  $t \in [0, 1]$  (Note:  $\mathbf{B}(\mathbf{x}, 0) = \mathbf{B}(\mathbf{a}, 0)$ ). The fluid flow map is a map  $\phi : R^3 \times [0, 1] \rightarrow R^3$  given by:

$$\phi_t : \mathbf{a} \mapsto \mathbf{x}$$

where  $\mathbf{a}$  denotes the initial position,  $\mathbf{x}$  denotes some final position, and  $t$  is in the interval  $[0, 1]$ .

The fluid flow map tracks the motion of every individual fluid particle as a function of time. We want to deal with ‘tame’ (see [3]) fluid flow maps, characterized by the following assumptions:

- (1) For all  $t \in [0, 1]$  the map  $\phi_t$  is a homeomorphism
- (2) The map  $\phi$  is ‘smooth’ and ‘volume preserving’

The smoothness of  $\phi$  implies that it is differentiable everywhere, hence it is continuous everywhere. In the case where  $\mathbf{B}$  encloses space (i.e. flux tubes), the ‘volume preserving’ condition forces volume to be an invariant under the evolution of the magnetic field. When we relax these assumptions, we get the formation of singularities and cusps, which we will avoid in this paper [3].

Suppose the magnetic field  $\mathbf{B}$  is solenoidal (i.e. zero divergence). Since the ‘solenoidal condition’ is satisfied, we can show that there exists a vector potential  $\mathbf{A}(\mathbf{x}, t)$  such that the divergence of  $\mathbf{A}$  is 0 and that  $\mathbf{B} = \nabla \times \mathbf{A}$  [2].

Notice how  $\mathbf{B}$  takes on the role of the vorticity field  $\omega$  and  $\mathbf{A}$  takes the job of the velocity field  $\mathbf{u}$  when compared to the equations from Section 3. Following Moffatt’s definition, the magnetic helicity is given as:

$$\mathcal{H}_M = \int \mathbf{A} \cdot \mathbf{B} dV \quad (5)$$

According to Moffatt, this equation describes how linked the magnetic field lines are in the conducting fluid. These lines are preserved via the ‘frozen field’ property, as we will now explain [1].

**Magnetic flux** is a measurement of the amount of magnetic field lines that pass through a given area, and is constant in a flux tube by virtue of the solenoidal condition [2]. Assume, much like we did for vorticity field lines, that the magnetic field is carried by the fluid with the constraint that its flux is conserved. Since there is a preservation of flux, the magnetic field is ‘frozen’ and satisfies:

$$\frac{\partial \mathbf{B}}{\partial t} = \nabla \times (\mathbf{u} \times \mathbf{B}) \quad (6)$$

Equation 6 resembles 3 with the magnetic field  $\mathbf{B}$  taking the role of the vorticity field  $\omega$ . Physically,  $\mathbf{B}$  is a magnetic field embedded in a fluid medium, and is continuously deformed due to the velocity field  $\mathbf{u}$ . Treating the magnetic field as a manifold, we can use the mathematics of continuum mechanics to show that there is a diffeomorphism between the initial and final field configurations.

**Theorem.** The frozen field equation defines a diffeomorphism between the initial and final magnetic field configurations.

*Sketch of Proof, from [3].* The solution to the frozen field equation (6), according to continuum mechanics, is

$$B_i(\mathbf{X}, t) = B_j(\mathbf{a}, 0) \frac{\partial X_i}{\partial a_j}$$

This equation explains the motion of the field from the initial position  $\mathbf{a}$  to its final configuration at  $\mathbf{X}$ . Furthermore, it explains the distortion via the deformation tensor  $\frac{\partial X_i}{\partial a_j}$ . According to Ricca, this tensor is a time-dependent map between the initial and final positions, defining a diffeomorphism [3]. We assume that the Jacobian determinant is 1 since the fluid is incompressible (i.e.  $\det(\frac{\partial X_i}{\partial a_j}) = 1$ ). So, in ideal MHD, the deformation of the magnetic field occurs by means of a diffeomorphism.  $\square$

Rather than looking at the deformation of the entire magnetic field, we can also place our focus on how flux tubes undergo deformation via the fluid flow map.

**Theorem.** The fluid flow map is an ambient isotopy of embedded flux tubes.

*Proof.* (From [3]) Recall that an ambient isotopy is a homotopy of homeomorphisms. Let  $\phi : R^3 \times [0, 1] \rightarrow R^3$  be the fluid flow map as defined earlier, which is continuous due to the smoothness property. By definition, for all  $t$  in  $[0, 1]$ ,  $\phi_t$  is a homeomorphism.

Let  $L_m$  be an embedding of a flux tube in  $R^3$  defined by the following two maps:

$$f : L_m \rightarrow R^3$$

$$g : L_m \rightarrow R^3$$

such that  $f$  and  $g$  are injective, continuous, and homeomorphisms when restricted to their image. By definition,  $\phi_0$  maps every particle's start point to the same start point. Since  $\phi_0$  is the identity,  $\phi_0 \circ f = f$ .

By Helmholtz's laws of vortex motion,  $\phi_1 \circ f(L_m) = g(L_m)$  (i.e. vortices are conserved in ideal fluid flow because there is no dissipation). Using this, we can show  $\phi_1 \circ f = g$ , meaning  $\phi$  is an ambient isotopy of flux tubes.  $\square$

## 5 Helicity and Linking Number

Consider a collection of flux tubes  $L_m$  for  $m = 1, 2, 3, \dots$  that are linked, and assume each tube is formed by the unknot. We can write helicity and flux, physical invariants of Euler evolution, alongside linking number, a knot invariant, together using the following formula [3]:

$$\mathcal{H}(L_m) = \sum_i Lk_i \Phi_i^2 + 2 \sum_{i \neq j} Lk_{i,j} \Phi_i \Phi_j \quad (7)$$

$Lk_{i,j}$  denotes the Gauss linking number of the  $i$ -th flux tube with respect to the  $j$ -th flux tube in the collection  $L_m$ . Since  $Lk_{i,j} = Lk_{j,i}$ , the factor of 2 appears in Equation 7. The  $Lk_i$  term denotes the Calugareanu-White linking number, which measures the 'self-linking' of each flux tube. Since we assume that every flux tube is formed via the unknot (i.e. every tube is unknotted), then each  $Lk_i$  is 0, and the equation simplifies to:

$$\mathcal{H}(L_m) = 2 \sum_{i \neq j} Lk_{i,j} \Phi_i \Phi_j \quad (8)$$

Performing computations will provide insight into the use of this equation.

**Example (Hopf Link).** Consider two flux tubes forming a Hopf link in Figure 8:

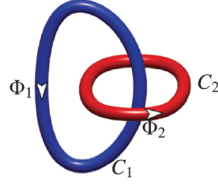


Figure 8: Flux Tubes in a Hopf Link, from [2]

Assume that each tube is formed by unknotted closed curves  $C_1$  and  $C_2$ . The linking number of the Hopf link of this orientation is 1, so

$$\mathcal{H} = 2Lk_{1,2}\Phi_1\Phi_2$$

$$\mathcal{H} = 2\Phi_1\Phi_2$$

Equation 7 alleviates the need to use the integral form of helicity in computations. Since the equation writes helicity as a function of linking number, it motivates the topological interpretation that helicity is a measure of the ‘linkedness’ of a vorticity field.

**Example (Whitehead Link).** Consider the Whitehead link formed by two flux tubes as shown in Figure 9:

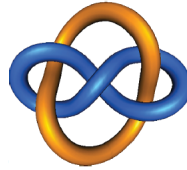


Figure 9: Flux Tubes in a Whitehead Link, from [2]

Suppose that each flux tube is made by unknotted closed curves. Recall from Section 2 that the linking number of the Whitehead link is 0. Since we assume the curves are unknotted, we use equation 8 and get:

$$\mathcal{H} = 2Lk_{1,2}\Phi_1\Phi_2$$

So,  $\mathcal{H} = 0$ . What this example implies is that while helicity is a measure of how linked the structure of the field is,  $\mathcal{H}$  can be 0 even if the field contains many links.

## 6 Energy Minimization Problem

In ideal MHD, magnetic fields embedded in a conducting fluid are considered ‘frozen’. We have shown that this ‘frozen’ property implies that the initial and final states of the magnetic field are related to each other via a diffeomorphism. Furthermore, we have proven that the deformation of the magnetic field, when treated as flux tubes, is an ambient isotopy. We know that linking number is an invariant of ambient isotopy, and that helicity is an invariant of Euler evolution, meaning they are both conserved in ideal MHD. Other physical properties such as volume and flux must also be conserved due to the assumptions made in ideal MHD.



We will now relax one of the assumptions of this paper and claim that the fluid medium can have internal friction. There is a magnetic potential energy  $M(t) = \frac{1}{2} \int \mathbf{B}^2 dV$  that gets converted to kinetic energy, which then gets distributed through the fluid due to viscosity.

**Theorem.** Assume  $\mathcal{H}_M \neq 0$ , then there is some positive lower bound to magnetic potential energy.

*Proof.* (From [2]) We start with the Cauchy-Schwarz inequality:

$$|\langle u, v \rangle| \leq \|u\| \|v\|$$

For  $u, v \in V$ , where  $V$  is some vector space. Let  $V$  be the real vector space  $R^3$ . Let  $\mathbf{a}, \mathbf{b} \in R^3$  be arbitrary vectors. Define the inner product as  $\langle \mathbf{a}, \mathbf{b} \rangle = \int \mathbf{a} \cdot \mathbf{b} dV$ . The CS inequality becomes:

$$\begin{aligned} \int \mathbf{A}^2 dV \int \mathbf{B}^2 dV &\geq \left( \int \mathbf{A} \cdot \mathbf{B} dV \right)^2 \\ &= \mathcal{H}_M^2 \end{aligned}$$

We also use the Poincare inequality (see [2] for derivation), which can be written as:

$$\int \mathbf{B}^2 dV \geq q^2 \int \mathbf{A}^2 dV$$

Where  $q > 0$  is some constant. Combining these inequalities, we get that:

$$\begin{aligned} \mathcal{H}_M^2 &\leq \frac{1}{q^2} \left( \int \mathbf{B}^2 dV \right)^2 \\ q|\mathcal{H}_M| &\leq \int \mathbf{B}^2 dV \end{aligned}$$

In the last step, we take the absolute value of helicity, negating the effects the projection has on the sign of  $\mathcal{H}$ . So, there exists a positive lower bound to  $M(t)$  dependent on magnetic helicity.  $\square$

The explanation of this phenomena ties in everything we have discussed in this paper so far. Suppose the magnetic field we are dealing with is a collection of flux tubes embedded in a conducting fluid medium. As the tubes relax, the magnetic field lines will shorten. Since volume must be conserved, the cross-sectional area of each tube will increase. However, since the deformation of flux tubes occurs via ambient isotopy, knot topology must be conserved. The conservation of topology ensures that as parts of the tube start to touch each other, the relaxation process stops to ensure the knot remains the same, explaining the existence of this lower bound.

## References

- [1] Keith Moffatt. *Helicity and singular structures in fluid dynamics*. PNAS, 111(10): 3663-3670, 2014.
- [2] Keith Moffatt and Emmanuel Dormy. *Self-Exciting Fluid Dynamos*. Cambridge University Press, New York, New York, 2019.
- [3] Renzo Ricca. *Applications of Knot Theory in Fluid Mechanics*. Mathematics Subject Classification, 76(02): 321-346, 1991.

- [4] Colin Adams. *The Knot Book: An Elementary Introduction to the Mathematical Theory of Knots*. American Mathematical Society, Providence, Rhode Island, 2004.
- [5] Keith Moffatt. *Knots and Fluid Dynamics*. 1998, DOI: 10.1142/9789812796073 \_ 0012.
- [6] Stephen Childress. *Topological Fluid Dynamics for Fluid Dynamicists*. Lecture Notes, Courant Institute of Mathematical Sciences, 2004.
- [7] Renzo Ricca and Mitchell Berger. *Topological Ideas and Fluid Mechanics*. Physics Today, 49(12): 28-34, 1996.
- [8] Robert Ghrist. *Elementary Applied Topology*. Ed. 1.0, Createspace, 2014.
- [9] Louis Kauffman. *An Invariant of Regular Isotopy*. Transactions of the American Mathematical Society, 318(2): 417-471, 1990.
- [10] John Lee *Introduction to Topological Manifolds*. Springer, New York, New York, 2011.